Available online at www.sciencedirect.com

SCIENCE DIRECT

Virology 334 (2005) 234–244

VIROLOGY

www.elsevier.com/locate/yviro

Distinct roles of enhancer nuclear factor 1 (NF1) sites in plasmacytoma and osteopetrosis induction by Akv1-99 murine leukemia virus

Karina Dalsgaard Sørensen[a], Annette Balle Sørensen[a], Leticia Quintanilla-Martinez[b], Sandra Kunder[b], Jörg Schmidt[c], Finn Skou Pedersen[a,d,*]

[a]*Department of Molecular Biology, University of Aarhus, C.F. Møllers Allé, Building 130, DK-8000 Aarhus C, Denmark*
[b]*Institute of Pathology, GSF-National Research Center for Environment and Health, Neuherberg, Germany*
[c]*Department of Comparative Medicine, GSF-National Research Center for Environment and Health, Neuherberg, Germany*
[d]*Department of Medical Microbiology and Immunology, University of Aarhus, Denmark*

Received 23 November 2004; returned to author for revision 30 December 2004; accepted 31 January 2005

Abstract

Murine leukemia viruses (MLVs) can be lymphomagenic and bone pathogenic. In this work, the possible roles of two distinct proviral enhancer nuclear factor 1 (NF1) binding sites in osteopetrosis and tumor induction by B-lymphomagenic Akv1-99 MLV were investigated. Akv1-99 and mutants either with NF1 site 1, NF1 site 2 or both sites disrupted induced tumors (plasma cell proliferations by histopathology) with remarkably similar incidence and mean latency in inbred NMRI mice. Clonal immunoglobulin gene rearrangement detection, by Southern analysis, confirmed approximately half of the tumors induced by each virus to be plasmacytomas while the remaining lacked detectable clonally rearranged Ig genes and were considered polyclonal; a demonstration that enhancer NF1 sites are dispensable for plasmacytoma induction by Akv1-99. In contrast, X-ray analysis revealed significant differences in osteopetrosis induction by the four viruses strongly indicating that NF1 site 2 is critical for viral bone pathogenicity, whereas NF1 site 1 is neutral or moderately inhibitory. In conclusion, enhancer NF1 sites are major determinants of osteopetrosis induction by Akv1-99 without significant influence on viral oncogenicity.

Keywords: Murine leukemia virus; Nuclear factor 1; Akv1-99; Oncogenesis; Pathogenicity; Plasmacytoma; Osteopetrosis

Introduction

Murine leukemia viruses (MLVs) are simple retroviruses, which can induce hematopoietic malignancies in mice. In addition, some MLVs hold a considerable potential for induction of bone lesions such as osteomas (benign bone tumors) (Luz et al., 1991) and osteopetrosis, a generalized disorder of the skeleton characterized by a significantly augmented bone mass, which in severe cases may completely fill the bone marrow cavity with osteoid, yet maintain the overall shape of the skeleton (Ethelberg et al., 1999; Murray et al., 1991; Schmidt et al., 1999). The condition seems to evolve primarily via osteoblast defects and secondarily via osteoclasts (Schmidt et al., 1999) and may therefore also be termed osteosclerosis (Whyte, 1996). MLV-induced osteopetrosis has always been found associated with tumor development (Ethelberg et al., 1999; Gimbel et al., 1996; Lovmand et al., 1998; Murray et al., 1991; Schmidt et al., 1984), but it is unclear if there is a coupling between the disease processes (Schmidt et al., 1999). In man, localized bone lesions (mostly lytic, rarely osteosclerotic) are common clinical features of multiple myeloma and adult T-cell leukemia and seem to develop in response to tumor cell-mediated effects in the bone marrow microenvironment (Mundy, 1997; Roodman, 1997).

Important genetic determinants of MLV lymphomagenicity have been mapped to the proviral U3 enhancer

* Corresponding author. Department of Molecular Biology, University of Aarhus, C.F. Møllers Allé, Building 130, DK-8000 Aarhus C, Denmark. Fax: +45 8619 6500.
E-mail address: fsp@mb.au.dk (F.S. Pedersen).

0042-6822/$ - see front matter © 2005 Elsevier Inc. All rights reserved.
doi:10.1016/j.virol.2005.01.039

(Celander and Haseltine, 1984; Chatis et al., 1984; DesGroseillers and Jolicoeur, 1984; Lenz et al., 1984), and in some cases to individual transcription factor binding sites (Hallberg and Grundström, 1988; Nieves et al., 1997; Speck et al., 1990); however, little is known about genetic determinants of MLV-induced bone disease. By using chimeras of highly bone pathogenic RFB MLV and T-lymphomagenic SL3-3 MLV non-LTR sequences were identified as major determinants of osteoma induction (Østergaard et al., 1997). Also, Runx (core/AML1) and nuclear factor 1 (NF1) binding sites in the enhancer of SL3-3 were found to be important for viral osteopetrosis induction (Ethelberg et al., 1999) with only the former playing a significant role also in lymphomagenesis (Ethelberg et al., 1997a; Hallberg et al., 1991).

Akv1-99 is an ecotropic MLV derived from endogenous Akv MLV of the AKR mouse by deletion of one copy of the 99-bp transcriptional enhancer in the proviral LTR (Lovmand et al., 1998). Both viruses induce B-cell lymphomas with high incidence and 12 months mean latency in random-bred NMRI mice (Lovmand et al., 1998). Akv is also significantly bone pathogenic (Gimbel et al., 1996; Luz et al., 1991; Murray et al., 1991; Schmidt et al., 1995), whereas reports of bone disease induction by Akv1-99 are rare (Lovmand et al., 1998) with no previous records of osteopetrosis. The 99-bp enhancer of Akv1-99 contains two distinct NF1 motifs, termed NF1 site 1 and 2, respectively. The NF1 site 2 sequence is a part of the conserved MLV enhancer framework (Golemis et al., 1990) and identical to the NF1 site present in three copies in the enhancer of SL3-3 MLV (Ethelberg et al., 1997a, 1997b, 1999; Hallberg et al., 1991; Nieves et al., 1997). NF1 factors bind to DNA as homo- or heterodimers, and numerous complexes with regulatory abilities ranging from activation to repression of transcription can be formed from several splice variants of the four NF1 family genes (Chaudhry et al., 1998; Gao and Kunos, 1998; Gronostajski, 2000; Kruse and Sippel, 1994; Mermod et al., 1989). NF1 site 1 is a stronger in vitro binding sequence than NF1 site 2 for a protein complex compatible with NF1 (Olsen et al., 1990), but the molecular interactions between NF1 motifs in Akv1-99 and NF1 proteins remain to be examined in detail with a possibility that these sites are recognized by other factors in vivo.

In this study, three different enhancer mutants of Akv1-99 were generated to investigate the function of NF1 site 1 and NF1 site 2 in viral lymphoma and osteopetrosis induction. The study was based on our previous identification of enhancer NF1 sites as major determinants of osteopetrosis but not T-cell lymphoma induction by closely related SL3-3 MLV (Ethelberg et al., 1999). We found that the two NF1 sites regulate Akv1-99 enhancer activity in a highly cell type-dependent manner, ranging from strong stimulation to moderate repression. Cell type-specific differences were also prominent at the level of viral pathogenicity, since Akv1-99 and three NF1 site mutant viruses induced plasmacytomas with similar incidence and latency, but showed markedly different osteopetrosis induction capacities. Interestingly, NF1 site 2 (identical to the SL3-3 NF1 site sequence) was critical for osteopetrosis induction, while NF1 site 1 was neutral or moderately inhibitory. Thus, the separate roles of enhancer NF1 sites in tumor and osteopetrosis induction are similar for SL3-3 and Akv1-99 despite the distinct cell type specificities of oncogenic transformation.

Results

NF1 sites regulate Akv1-99 enhancer activity in a cell type-specific manner

To investigate the role of NF1 binding sites in transcriptional regulation of Akv1-99, enhancer reporter constructs with wild-type or mutated NF1 motifs were tested in transient expression assays in MPC11 B-cells, NALM6 pre-B-cells, L691 T-cells, MC 3T3 osteoblast-like cells and KM1/K3 osteoblast progenitor cells. NIH 3T3 fibroblasts were included as non-hematopoietic, non-bone mesenchymal cells known to contain NF1 site binding proteins in abundance (Goyal et al., 1990). The reporter plasmid p1-99(wt)-cat (Lovmand et al., 1990) harbors a complete Akv1-99 LTR to drive expression of a chloramphenicol acetyltransferase (CAT) reporter gene. The mutated constructs p1-99(m1)-cat, p1-99(m2)-cat and p1-99(dmNF1)-cat have substitutions in either NF1 site 1 or 2, or in both NF1 sites simultaneously (Fig. 1). Both half sites of the palindromic NF1 motifs were mutated to completely abolish in vitro binding of a protein complex with NF1 properties (Lovmand, 1996; Olsen et al., 1990). In the previous study, SL3-3 NF1 site mutants had a single 3-bp mutation in the upstream half site (Ethelberg et al., 1999).

Transient expression results are shown in Table 1 with average CAT activities of the different experiments given relative to the mean CAT activity measured for a similar expression vector, pAkv6cat (Lovmand et al., 1990), with two copies of the wild-type 99-bp enhancer sequence. The two NF1 sites were functionally indistinguishable in this assay, since p1-99(m1)-cat and p1-99(m2)-cat gave similar results in each of the six cell lines tested. In all cases, the effect of mutating two rather than one NF1 motif was largely additive. Disrupting both NF1 sites reduced CAT expression 10-fold in NIH 3T3 fibroblasts, consistent with the high levels of NF1 binding activity in this cell line (Goyal et al., 1990). The clearly most dramatic effects of NF1 site mutations, however, were seen in MC 3T3 and KM1/K3 osteoblastic cells in which mutation of both NF1 sites lowered Akv1-99 enhancer activity approximately 30-fold. These results suggest that enhancer NF1 motifs are of major importance for expression of Akv1-99 in osteoblasts and osteoblast precursor cells and may influence the osteopetrosis induction potential of the virus.

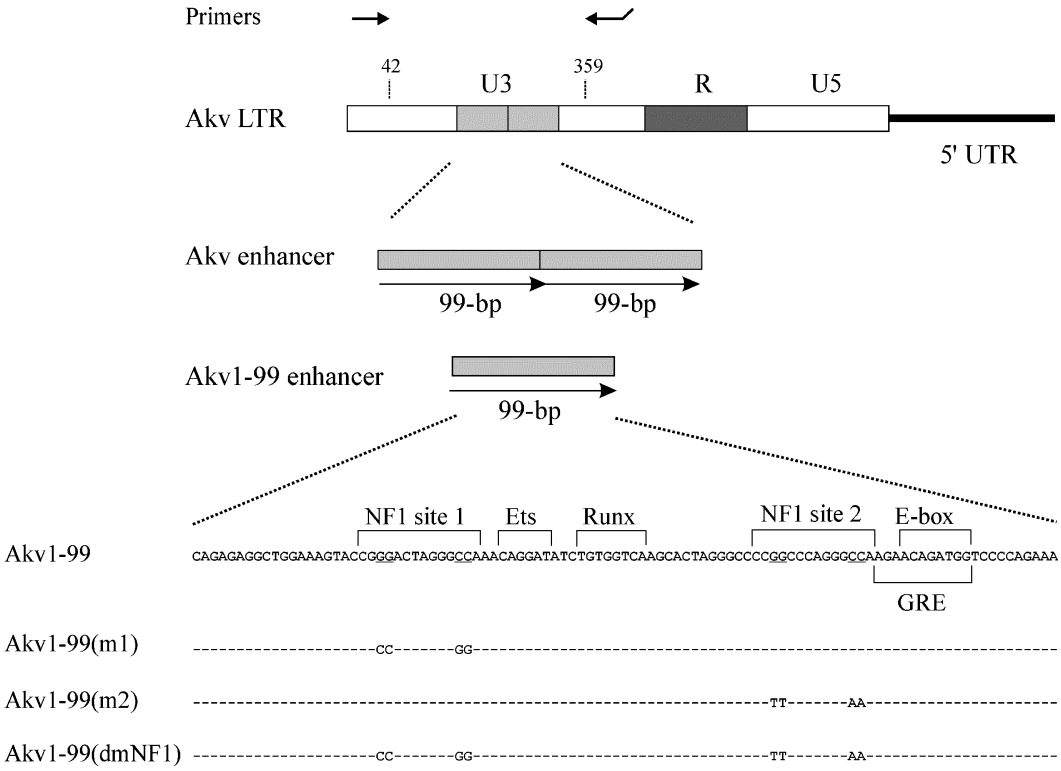

Fig. 1. LTR and enhancer structures of Akv and Akv1-99. The 99-bp tandemly duplicated transcriptional enhancer of Akv is present in only one copy in the U3 region of Akv1-99. The 99-bp enhancer sequence contains two distinct nuclear factor 1 (NF1) transcription factor binding sites, NF1 site 1 and 2, respectively, besides an Ets site, a Runx site, an E-box site and a glucocorticoid response element (GRE). NF1 site 2 is also referred to as the enhancer framework NF1 site. Point mutations introduced into the NF1 sites of Akv1-99-based CAT expression plasmids or provirus constructs are shown at the bottom. The primer pair used for PCR amplification of proviral U3 regions is shown at the top. 5′ UTR, 5′ untranslated region.

CAT expression levels were reduced 6-fold in MPC11 plasmacytoma B-cells and 4-fold in NALM6 pre-B-cells when both NF1 sites were mutated. Although this indicates that the NF1 sites stimulate Akv1-99 enhancer activity in the lymphoid target cells of Akv1-99, and thereby may contribute to viral oncogenicity, we note that the impact of NF1 site mutations was much less pronounced in the hematopoietic cell lines than in the osteoblastic cell lines used here. Finally, the transient assays showed that NF1 sites are weak negative regulators of Akv1-99 enhancer activity in L691 T-cells, as evident only when two sites were mutated simultaneously.

Together with earlier work (Ethelberg et al., 1997a, 1999; Olsen et al., 1990), this study revealed similar regulatory roles for NF1 sites in viral transcriptional control in the five different cell lines, MPC11, L691, NIH 3T3, MC 3T3 and KM1/K3, regardless of their location being in the enhancer context of B-lymphomagenic Akv1-99 or T-lymphomagenic SL3-3. In both cases, viral enhancer activity was up-regulated via intact NF1 binding sites in the B-lymphoid and osteoblastic cell lines, but down-regulated in L691 T-cells. Hence, the varying CAT activities measured for pAkv6cat versus p1-99(wt)-cat in NALM6, L691, NIH 3T3, MC 3T3 and KM1/K3 cells (Table 1) may at least in part be explained by different numbers of NF1 motifs in the U3 enhancers. No effect of repeat number variation was seen in MPC11 cells, probably due to involvement of other factors.

Table 1
Results of transient expression experiments

Expression vector	Relative CAT activity (SD)[a]					
	MPC 11	NALM6	L691	NIH 3T3	MC 3T3	KM1/K3
pAkv6cat	100	100	100	100	100	100
p1-99(wt)-cat	101 (22)	41 (11)	193 (24)	52 (20)	65 (18)	26 (9)
p1-99(m1)-cat	24 (6)	23 (9)	150 (31)	12 (5)[b]	9 (4)	2 (0.6)
p1-99(m2)-cat	28 (11)	23 (6)	205 (79)	15 (6)	5 (2)	3 (2)
p1-99(dmNF1)-cat	16 (11)	10 (5)	318 (50)	5 (3)	2 (0.8)	1 (0.8)

[a] Transient transfection assays with CAT reporter constructs. The average CAT activities are normalized to the activity of Akv6cat, which was arbitrarily set to 100. Standard deviations of 3–11 independent transfections are given in parentheses. All transfections were performed in duplicate.
[b] We note that the quantification of Akv1-99(m1) LTR-driven CAT expression in NIH 3T3 cells repeats and confirms earlier work (Olsen et al., 1990).

NF1 sites are dispensable for plasmacytoma induction by Akv1-99

To investigate the role of enhancer NF1 sites for viral oncogenicity, infectious Akv1-99 virus particles with mutations in NF1 site 1, NF1 site 2 or both NF1 sites were injected into newborn inbred NMRI mice together with wild-type Akv1-99. Akv1-99 and the three mutant viruses induced tumors with remarkably similar incidence and mean latency periods of 6 months (Fig. 2; Table 2).

The morphological changes observed in the lymphoid organs of mice infected with any of the four viruses were very similar. Cervical and mesenteric lymph nodes were significantly enlarged and revealed a complete effacement of the normal architecture by a diffuse and sometimes vaguely nodular proliferation (Fig. 3A). At higher magnification, most of the nodules were composed of a monotonous infiltration of medium-sized plasma cells with abundant cytoplasm, eccentric nuclei, and marginated chromatin (Fig. 3B). Hyperplastic germinal centers were identified in some areas (Fig. 3C). The germinal centers had ill-defined borders, abundant tingible-body macrophages and lacked well-formed mantle and marginal zones (Fig. 3C). In addition to the lymph nodes, the spleen was also infiltrated with expansion of the white pulp (Fig. 3D). Extramedullary hematopoiesis in the spleen was always present. Histologically, a diagnosis of plasma cell proliferation (consistent with plasmacytoma, i.e. plasma cell lymphoma) was made in all cases.

Macroscopically, an enlarged thymus was identified in only three cases; however, in many instances the medulla was infiltrated by the plasma cell proliferation (Fig. 3E). In some cases, the liver revealed an infiltrate in the portal tracts (Fig. 3F). Immunostaining for CD79a confirmed the B-cell nature of the residual follicles (Figs. 3G–H) and highlighted the typical plasma cell morphology of the infiltrate. Intermingled small reactive T-lymphocytes were positive for CD3 (not shown). TdT was negative in all cases (not shown), excluding the possibility of a pre-B lymphoblastic lymphoma.

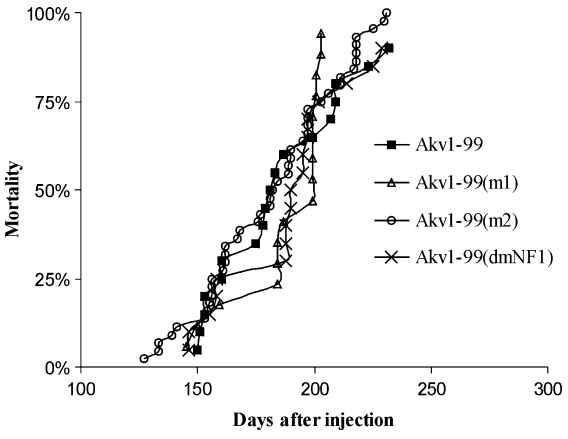

Fig. 2. Tumor induction in inbred NMRI mice injected with Akv1-99 or NF1 site-mutated viruses. The cumulative mortality is given as a function of the latency time.

Table 2
Tumor and osteopetrosis induction in inbred NMRI mice

Virus	Tumor incidence[a]	Mean tumor latency in days (SD)	Osteopetrosis incidence[b]
Akv1-99	19/20 (95%)	186 (28)	12/20 (60%)
Akv1-99(m1)	16/17 (94%)	187 (19)	13/17 (76%)
Akv1-99(m2)	44/44 (100%)	182 (28)	0/44 (0%)
Akv1-99(dmNF1)	18/20 (90%)	187 (25)	3/20 (15%)[c]
Mock[d]	1/21 (4.8%)	ND[e]	0/21 (0%)

[a] No. of mice with tumors/no. of injected mice. Within a 1-year observation period.
[b] As determined by X-ray analysis.
[c] Significantly different from Akv1-99 ($P < 0.05$), Akv1-99(m1) ($P < 0.005$) and p1-99(m2) ($P < 0.05$) (Fischer's exact test, two tailed).
[d] The mock-injected controls (data from Ethelberg et al., 1999) belonged to the same colony of inbred NMRI mice as the virus-injected mice, and were kept in the same facility.
[e] ND, not determined.

For further characterization, Southern blotting analysis of genomic tumor DNA was performed with hybridization probes derived from the immunoglobulin kappa light chain (Igκ), immunoglobulin heavy chain (IgH) and T-cell receptor β (TCRβ) loci. The molecular analyses did not reveal any significant differences between tumors induced by Akv1-99 and the three NF1 site mutants (Table 3; Fig. 4). Clonal Igκ and IgH gene rearrangements were detected in approximately one half of the mice infected with either of the four viruses, consistent with plasmacytoma. In five mice, weak TCRβ gene rearrangements were detected with the J2 but not the J1 probe; however, these tumors also had mono- or oligoclonal Igκ and IgH gene rearrangements (Fig. 4A, no. 3, 9–10; Fig. 4C, no. 8; and data not shown), altogether in support of a B-cell rather than a T-cell tumor phenotype. Unexpectedly, in a few tumors of each series, clonal DNA rearrangements were detected in only one of the analyzed Ig loci (Fig. 4D, tumor 3, and data not shown). There was no morphological evidence of a pre-B cell lymphoma phenotype in the tumors showing rearrangement of IgH but not Igκ, and it is possible that at least some of them have the lambda rather than the kappa light chain gene clonally rearranged.

In the remaining one half of the mice injected with each virus, no clonal rearrangements were detected in the three genes investigated by Southern analysis (Table 3; Fig. 4). Following the recommendations of the 2002 Bethesda mouse lymphoma classification system (Morse et al., 2002), and in the absence of morphological evidence of a null lymphoma phenotype, these cases were considered polyclonal. Although we cannot formally prove that the polyclonal plasma cell proliferations are malignant B-cell tumors, it is notable that histologically these cases could not be distinguished from the plasmacytomas with detectable Ig rearrangements and in all cases developed with similar mean latency.

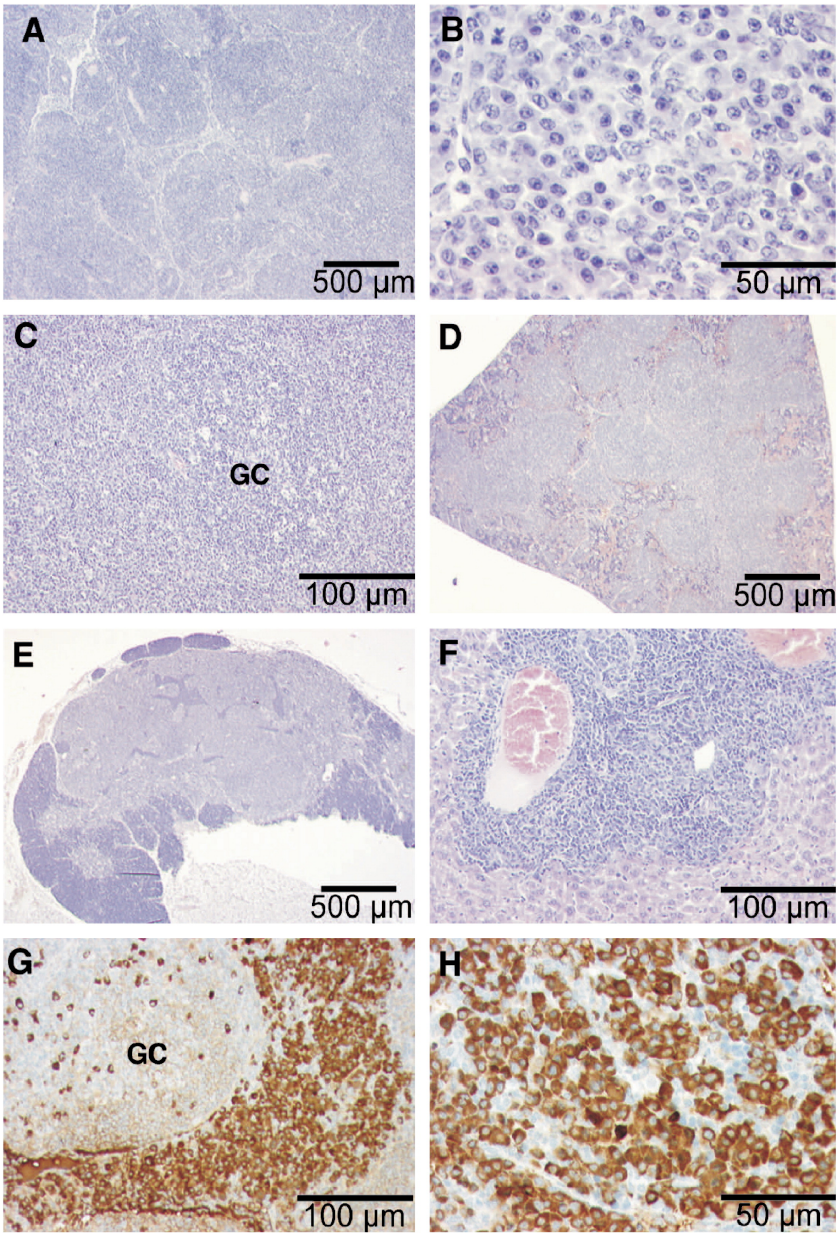

Fig. 3. Histological appearance of tumors induced by wild-type and NF1 site-mutated Akv1-99 viruses. (A) Mesenteric lymph node in a mouse infected with wild-type Akv1-99 MLV. The normal architecture of the lymph node is effaced by a nodular proliferation of medium-sized plasma cells (hematoxylin and eosin). (B) Mesenteric lymph node in a mouse infected with Akv1-99(m1). The lymph node is diffusely infiltrated by a monotonous proliferation of medium-sized plasma cells with abundant cytoplasm, eccentric nuclei and marginated chromatin. Occasionally a small nucleolus is identified (hematoxylin and eosin). (C) Mesenteric lymph node in a mouse infected with Akv1-99(m1). The lymph node is diffusely infiltrated by plasma cells. There is partial preservation of the lymph node architecture with ill-defined germinal centers (GC) that show a starry sky pattern and lack mantle zones (hematoxylin and eosin). (D) Spleen in a mouse infected with Akv1-99(m1). The white pulp of the spleen is expanded by a vaguely nodular infiltrate composed of medium-sized plasma cells. Rare residual germinal centers are identified. Note the intense erythropoiesis in the subcapsular area (hematoxylin and eosin). (E) Thymus in a mouse infected with Akv1-99(dmNF1). The medulla of the thymus is expanded by a proliferation of plasma cells. Note that the cortical area is compressed (hematoxylin and eosin). (F) Liver in a mouse infected with Akv1-99(m1). The liver shows a marked infiltrate in the portal tracts surrounding blood vessels and bile ducts (hematoxylin and eosin). (G) Mesenteric lymph node stained with anti-CD79a. The B-cells in the germinal center (GC) show a specific membranous staining. The strong staining of cytoplasmic immunoglobulin by the secondary antibody highlights the typical plasma cell morphology surrounding the GC (immunohistochemistry). (H) Higher magnification of a nodule composed almost exclusively of plasma cells (immunohistochemistry).

These results show that enhancer NF1 site sequences are dispensable for plasmacytoma induction by Akv1-99. Hence, the significant effects on viral enhancer activity measured in two B-lymphoid cell lines, including a murine plasmacytoma cell line (MPC11), after mutating one or both NF1 site(s) (Table 1) were not manifested at the level of viral tumorigenicity. We note that the lymphoma latency period of Akv1-99 was significantly shorter in inbred NMRI mice, as shown here, than in random-bred NMRI mice, as reported earlier (Lovmand et al., 1998). This may mask small

Table 3
Molecular tumor characterization

Virus	No. of mice with tumor development	DNA rearrangements[a]				Lymphoma incidence[b]
		Igκ	IgH	TCRβ-J1	TCRβ-J2	
Akv1-99	19	9/17	11/16	0/10	3/10	11/18
Akv1-99(m1)	16	5/11	8/14	0/10	0/12	9/15
Akv1-99(m2)	44	9/16	8/16	0/16	2/16	9/16
Akv1-99(dm)	18	9/18	4/11	0/10	0/14	11/18

[a] As determined by Southern blotting analysis of genomic tumor DNA with Ig- and TCRβ-specific hybridization probes (Igκ, IgH, TCRβ-J1 and -J2). No. of tumors with clonal rearrangements/no. of tumors investigated.
[b] Incidence of malignant lymphoma with clonal Ig gene rearrangements. No. of mice with clonal Ig gene rearangements detected/no. of mice analyzed. In a few cases, data was available for only one of the Ig chain genes.

differences in the lymphomagenic properties of the four viruses.

Proviral enhancer sequences were conserved in tumor DNA

Structural alterations or secondary mutations in the proviral enhancer region may arise in vivo and influence viral pathogenicity. To determine if the viral enhancers were genetically stable during lymphoma induction, proviral U3 regions were PCR amplified from genomic tumor DNAs of 69 mice, equally representing the four different viruses, by using a primer in the 5′ end of the U3 and a primer located ca. 60-bp downstream of the 99-bp enhancer element (Fig. 1). In all cases, only a single band of the size (277-bp) expected from the U3 structures of the input viruses was seen (data not shown), ruling out that major fluctuations in enhancer repeat copy numbers had occurred during viral tumor induction. Bulk sequencing of the PCR products (from nucleotide positions 42 to 260 of the viral LTRs) showed that the introduced NF1 site point mutations were always maintained, and that the wild-type enhancer sequence also had not changed. Second-site mutations were not discovered. This pronounced in vivo stability correlates well with the limited role of NF1 sites for Akv1-99 lymphomagenicity, most probably resulting in a minimum selection force against the mutated enhancers during tumorigenesis.

NF1 site 2 is a major determinant of osteopetrosis induction by Akv1-99

The bone pathogenic properties of wild-type or NF1 site-mutated Akv1-99 were evaluated by X-ray analysis of all deceased mice using the increase in cancellous bone mass, marked trabecular thickening, and loss of marrow cavity as characteristics of osteopetrosis (Ethelberg et al., 1999; Luz et al., 1991; Murray et al., 1991; Schmidt et al., 1999). This is a fast and reliable method for detection of MLV-induced osteopetrosis and, as previously shown in details, is well correlated with results obtained by laborious histological analyses, although the sensitivity of the latter is higher (Ethelberg et al., 1999; Murray et al., 1991; Schmidt et al., 1999).

By X-ray analysis, we found that the osteopetrosis induction potentials of the four viruses differed markedly. Akv1-99 induced osteopetrosis in 60% of the mice (Table 2). Mutation only of NF1 site 1 had no significant effect on viral bone pathogenicity, but radiologically detectable osteopetrosis induction was completely abolished by mutation only of NF1 site 2 (Table 2), strongly indicating a pivotal role of NF1 site 2 but not NF1 site 1 for induction of the skeletal lesion. The double mutant induced osteopetrosis in 15% of the mice (Table 2), showing that NF1 site 2 is not strictly required for osteopetrosis induction by Akv1-99. It also indicates that NF1 site 1 at least to some extent may inhibit viral bone pathogenicity, although this was not statistically significant by comparison of Akv1-99 and Akv1-99(m1).

The transient enhancer activities of wild-type and NF1 site-mutated Akv1-99 measured in MC 3T3 and KM1/K3 cells (Table 1) did not correlate well with the osteopetrogenic potencies of the corresponding viruses in inbred NMRI mice, although the two weakly bone pathogenic mutants both exhibited severely reduced enhancer strengths in the osteoblastic cell lines. This pattern is similar to our earlier findings for NF1 site mutants of SL3-3 (Ethelberg et al., 1999).

The present study is the first to identify an osteopetrosis induction potential by Akv1-99, which did not induce radiologically detectable osteopetrosis in random-bred NMRI mice, although osteomas developed with low incidence (Lovmand et al., 1998). None of the inbred NMRI mice infected with Akv1-99, Akv1-99(m1) or Akv1-99(dmNF1) had osteomas at the time of lymphoma development. This was not investigated for Akv1-99(m2). It is possible that the shorter tumor latency in inbred NMRI mice does not allow sufficient time for osteoma development, but the differences may rely also on other mouse strain specific factors.

Discussion

In this study, we have identified enhancer NF1 sites as major genetic determinants of osteopetrosis but not plasmacytoma induction by Akv1-99 MLV. NF1 site 1 was neutral

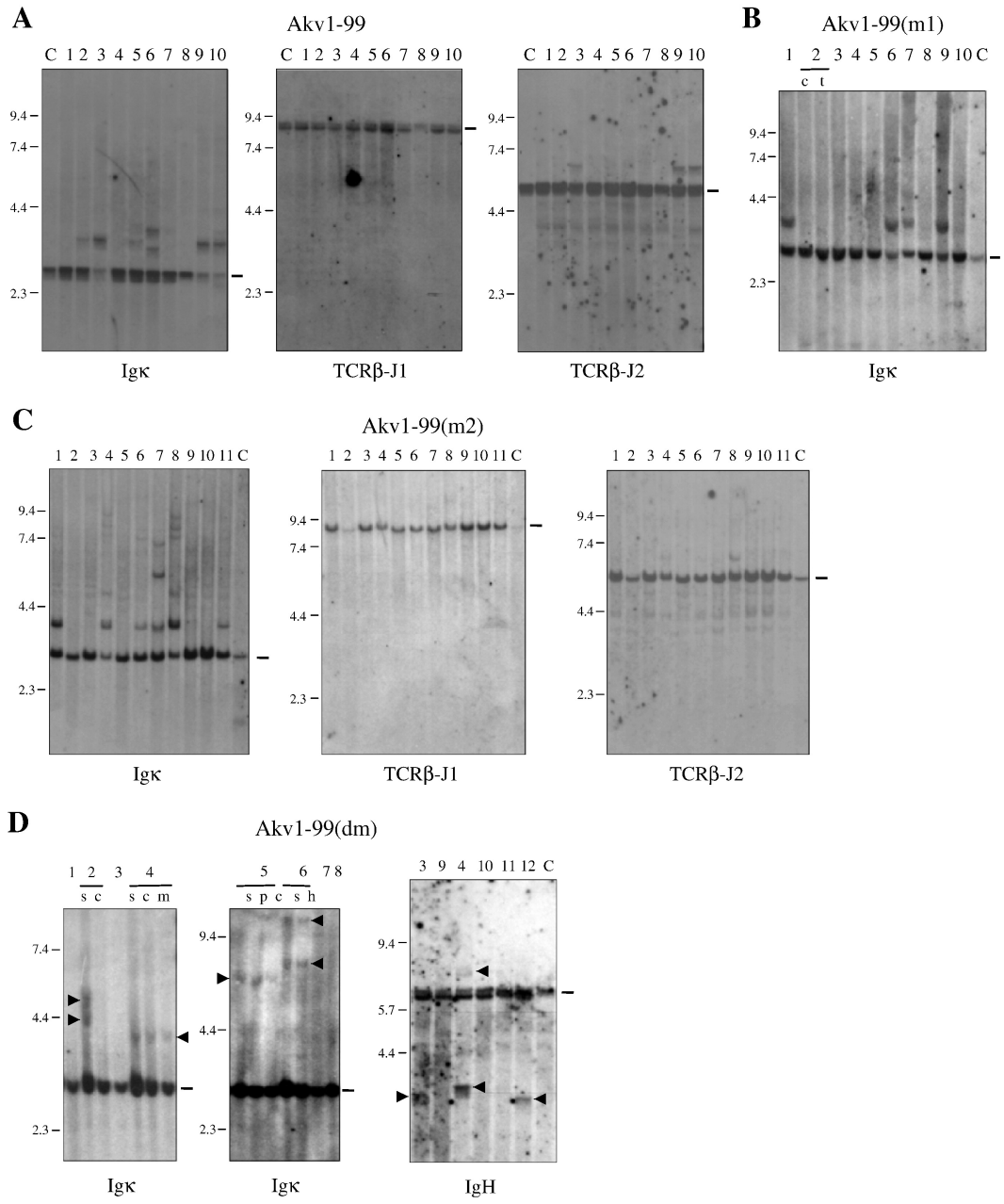

Fig. 4. Tumor characterization by Southern hybridizations. Genomic DNA from tumors induced by Akv1-99 (A), Akv1-99(m1) (B), Akv1-99(m2) (C) and Akv1-99(dmNF1) (D) was cleaved by *Hind*III and hybridized with the Igκ, TCRβ-J1 or TCRβ-J2 probes, or cut with *Eco*RI for hybridization with the IgH probe. Tumor numbers are given above each lane. (C) gDNA from a non-injected control mouse. In some cases, more than one tumor tissue was analyzed from the same mouse as indicated by one-letter abbreviations (c, cervical lymph node; m, mesenteric lymph node; p, para-aortic lymph node; s, spleen; t, thymus). Size markers (kb) are shown to the left of each blot. Black bars indicate the positions of genomic germline fragments. Some weak rearranged bands are highlighted by arrows.

or moderately inhibitory for virus-induced osteopetrosis development, whereas NF1 site 2 was critical though not absolutely essential. Hence, the divergent functions of the enhancer framework NF1 site sequence in viral tumor versus osteopetrosis induction are similar for Akv1-99 MLV, as shown here, and SL3-3 MLV, as reported earlier (Ethelberg et al., 1999), despite distinct cell type specificities of oncogenic transformation and differences between the exact point mutations used. The limited role of NF1 sites in lymphoma induction by Akv1-99 and SL3-3 may be a characteristic trait of Akv family viruses and contrasts a significant attenuation of T-lymphomagenesis by MoMLV upon mutation of an enhancer NF1 site present in two copies (Speck et al., 1990).

Reports of lymphoma induction by exogenous Akv or Akv1-99 are relatively rare (Lovmand et al., 1998; Speth et al., 1995), but several studies have pointed to a role of activated endogenous Akv in spontaneous models, includ-

ing B-cell lymphoma development in NFS.V$^+$ congenic mice (Hartley et al., 2000) and some AKXD strains (Gilbert et al., 1993; Mucenski et al., 1986, 1987). Expression of an endogenous ecotropic MLV, which may be identical to Akv (Jenkins et al., 1982; Yamada et al., 1994), is critical for the occurrence of pre-B-cell lymphomas in SL/Kh mice (Yamada et al., 1994). The ecotropic *emv*-1 locus, harboring a U3 sequence that differs from Akv1-99 only at a single position upstream of the enhancer (Lawrenz-Smith et al., 1994), may contribute to B-cell lymphomagenesis in CWD and SEA/GnJ mice (Angel and Bedigian, 1984; Mucenski et al., 1988), but seems not to be important for pristane-induced plasmacytomas in BALB/c mice (Potter and Wax, 1983; Potter et al., 1984).

Interestingly, the tumors induced by Akv1-99 and the three NF1 site mutants in inbred NMRI mice were plasmacytomas, while Akv1-99 induced only less differentiated types of B-cell malignancies (mostly B-cell lymphoblastic lymphoma) in random-bred NMRI mice (Lovmand, 1996; and unpublished results). We note that in inbred NMRI mice several independent tumors displayed rearranged fragments of similar size when analyzed by Southern blotting with the Ig kappa and Ig heavy chain probes (Fig. 4, and data not shown), a pattern not observed in random-bred NMRI mice (Lovmand et al., 1998). Such fragments were never seen in samples from negative controls of the same inbred NMRI colony and are therefore unlikely to represent odd cases of incompletely digested DNA samples.

Although comigration of fragments does not prove identity, it raises the possibility that Ig rearrangements are restricted in the tumors, further indicative of antigenic stimulation playing a key role in tumorigenesis. Repetitive usage of certain Ig gene segments occurs in spontaneous CD5$^+$ (B1) B-cell lymphomas in old mice of some strains (Rosner et al., 1993; Stall et al., 1988) and in young autoimmune NZB mice (Stall et al., 1988; Tarlinton et al., 1988). B1-cells in the peritoneal cavity (Stall et al., 1988) may be easily accessible for MLV infection upon ip inoculation, as performed here, and have also been suggested as possible precursors of pristane-induced plasmacytomas in the BALB/c mouse model (Potter and Wiener, 1992), which seems to require antigenic stimulation (Byrd et al., 1991). In man, restricted usage of Ig variable region sequences has been found in plasmacytomas associated with hepatitis C virus (HCV) infection (Gasparotto et al., 2002), and despite some controversy, there is increasing evidence for a role of HCV antigen-driven clonal B-cell expansion in at least some B-cell lymphoproliferative disorders (Weng and Levy, 2003).

We speculate that in the current model, MLV-induced plasmacytomas develop through a sequential process involving a benign restricted lymphoid expansion (hyperplasia), followed by an oligoclonal phase, which ultimately may lead to a monoclonal neoplastic proliferation (frank plasmacytoma). Antigenic stimulation from opportunistic infections might play a role during one or more of these steps, still only one of the mock-injected mice presented with signs of illness within the 1-year observation period, proving the essential role of MLV infection for tumorigenesis. An oligoclonal expansion is detectable by Southern analysis only if the proliferating population has reached a sufficient size and may explain the absence of clonal Ig gene rearrangements in half of the virus-injected mice. In many, but not all, positive cases the rearranged Ig bands were relatively weak (Fig. 4 and data not shown), which together with the highly similar histological observations for all investigated mice is consistent with the model of gradual progression from polyclonal plasma cell proliferation toward mono- or oligoclonal plasmacytoma. The most common human plasma cell malignancy, multiple myeloma, is usually if not always preceded by a benign plasma cell proliferation (monoclonal gammopathy of undetermined significance) (Kuehl and Bergsagel, 2002).

Although enhancer NF1 sites were dispensable for tumor induction by Akv1-99, this study unveiled a pivotal role of these sequences in viral osteopetrosis induction. One may speculate that NF1 site 1 is recognized by a protein complex that represses proviral transcription, whereas NF1 site 2 is bound by a complex that activates transcription in cell type(s) that must be productively infected in the process of osteopetrosis induction. It is even possible that the two sites are recognized by the same complex, which could have a down-regulatory function when bound to NF1 site 1 and an up-regulatory function when bound to NF1 site 2. Transient expression results indicated that NF1 sites are particularly important for sustaining high viral gene expression levels in osteoblastic cells, as compared to lymphoid cells. Hence, NF1 motifs may determine Akv1-99 osteopetrosis induction at least partly through regulation of viral protein expression in bone forming cells, but we found no simple correlation between viral enhancer strengths in the two osteoblastic cell lines MC3T3 and KM1/K3 and the osteopetrosis induction potential of the corresponding Akv1-99 viruses. Albeit representing different stages of osteoblastic differentiation these cell lines may not be representative of the host cell(s) targeted by Akv1-99 during osteopetrosis induction. Moreover, NF1 proteins can regulate transcription by mechanisms involving chromatin remodeling (Gronostajski, 2000), a regulatory level most likely not reflected in the transient assays. Likewise, there was no linear correlation between wild-type and NF1 site mutant SL3-3 transient enhancer activities in these bone cell lines and viral bone pathogenicity (Ethelberg et al., 1999).

The mechanism of viral osteopetrosis induction is still unknown. It may develop independently of tumorigenesis (Schmidt et al., 1999) or be caused by direct viral effects on bone cells along with indirect effects mediated by virus-induced (pre)leukemic cells in the bone marrow microenvironment. Furthermore, the fact that MLV-induced osteopetrosis seems only to develop in bones containing bone marrow (Murray et al., 1991) may reflect the existence

of a complicated interplay between virus, bone cells, hematopoietic cells and bone marrow stromal cells. Finally, the incidence of osteopetrosis in MLV-infected animals might be affected by stochastic factors if a series of events is needed to disrupt balanced bone remodeling. Each event may not always occur or the events may not necessarily appear in the required combination. In conclusion, this work has provided novel mouse models of plasmacytoma development, which are well-suited for future studies also investigating potential pathophysiological effects on other cell types than the target cells of oncogenic transformation, in particular bone lesions as commonly seen in human malignancies such as multiple myeloma.

Materials and methods

Cell culture

MPC11 murine plasmacytoma B-cells, L691 murine T-lymphoid cells, NIH 3T3 murine fibroblast cells and the murine osteoblastic cell lines MC 3T3 (Sudo et al., 1983) and KM1/K3 (Werenskiold et al., 1995) were grown as previously described (Ethelberg et al., 1997a, 1999). NALM6 human pre-B-cells (Hurwitz et al., 1979) were grown in RPMI 1640 medium with Glutamax-1 (Gibco BRL, Invitrogen Corporation), supplemented with 10% newborn calf serum, 100 U/ml penicillin and 100 μg/ml streptomycin.

Plasmids

Chloramphenicol acetyl transferase (CAT) expression vectors pAkv6cat and p1-99(wt)-cat have been described previously (Lovmand et al., 1990), p1-99(m1)-cat is identical to pM4 (Olsen et al., 1990), p1-99(m2)-cat was provided by Dr. Jette Lovmand (Lovmand, 1996) and p1-99(dmNF1)-cat was generated by exchanging an *Apa*I–*Kpn*I fragment between p1-99(m1)-cat and p1-99(m2)-cat. The proviral clone of Akv1-99 harbors the complete viral genome with one entire but permuted LTR (Lovmand et al., 1998). Akv1-99 provirus plasmids with mutated NF1 site(s) were made by substitution of a U3 containing *Pvu*I–*Pvu*I fragment from the wild-type Akv1-99 proviral clone with an equivalent *Pvu*I–*Pvu*I fragment from p1-99(m1)-cat, p1-99(m2)-cat and p1-99(dmNF1)-cat, respectively.

Generation of viruses

Infectious virus particles were produced as previously described. In short, concatemerized *Pst*I–*Pst*I fragments of the proviral plasmid clones were transfected into NIH 3T3 cells (Ethelberg et al., 1997b; Lovmand et al., 1998), virus production was monitored by RT assays (Hallberg et al., 1991) and the LTR regions of proviruses were amplified from virus producing NIH 3T3 cells by PCR and sequenced (see below) to confirm the integrity of the mutations.

Pathogenicity experiments and histopathological examination

10^5 to 10^6 infectious virus particles, as measured by infectious center assays (Schmidt et al., 1988), were injected intraperitoneally into newborn inbred NMRI mice, which do not harbor endogenous ecotropic MLVs (Leib-Mösch et al., 1986). Control mice from the same colony were mock injected with complete medium. The mice were checked for tumor development 5 days a week and sacrificed when they showed signs of illness. Tumor development was diagnosed on the basis of grossly enlarged lymphatic organs after having reached the size described earlier, which is compatible with lymphoma (Schmidt et al., 1984). Histological examination of hematoxylin and eosin (H&E)-stained sections from formalin-fixed and paraffin-embedded lymphoid organs was carried out for representative animals of each group. Tumors were classified according to the Bethesda proposals for classification of lymphoid neoplasms in mice (Morse et al., 2002). Immunohistochemistry was performed on an automated immunostainer (Ventana Medical System, Inc.; Tucson, AZ), according to the protocol provided by the company. The antibody panel used included polyclonal anti-CD3, anti-CD79a and anti-TdT (Dako; Denmark). Osteopetrosis was diagnosed by X-ray analysis. Positive cases were determined by a thickening of bone trabecules and of the cortex together with a loss of the spongious structure in the vertebrae and/or a loss of the marrow cavity in other bones. Particular attention was put to the primary sites of osteopetrosis, including the iliac crest, the lower part of the lumbar vertebral column, ends of the ribs, the distal femur and the proximal tibia. The analyses were based on previous studies, which have shown in detail that osteopetrosis is readily detected by X-ray (Ethelberg et al., 1999; Murray et al., 1991; Schmidt et al., 1999). Statistical calculations were carried out using the two-tailed Fisher's exact test.

Southern blotting analyses

Genomic DNA was extracted from frozen tumor tissues using the DNeasy Tissue Kit (Qiagen). Southern blotting and hybridizations with ^{32}P random priming labeled probes were performed as earlier (Ethelberg et al., 1997b). Hybridization probes used with *Hind*III-digested gDNA included immunoglobulin kappa light chain (Igκ) and T-cell receptor β gene-specific probes TCRβ-J1 and TCRβ-J2. Furthermore, tumor DNAs were analyzed with an Ig heavy chain specific probe (termed IgH-J11) after *Eco*RI digestion. All probes were as previously described (Lovmand et al., 1998).

Transfections and reporter assays

MPC11, NALM6 and L691 were transfected by the DEAE-dextran method (Ethelberg et al., 1997a), while NIH 3T3, MC 3T3 and KM1/K3 cells were transfected by

calcium phosphate-mediated precipitation (Ethelberg et al., 1997a). For each transfection, 4 μg (MPC11 and L691) or 3 μg (NALM6, NIH 3T3, MC 3T3 and KM1/K3) CAT expression vector was used together with 1.0 μg (MC 3T3 and KM1/K3), 1.5 μg (L691 and NIH 3T3) or 2.0 μg (MPC11 and NALM6) of pRSV-luc (Promega) internal control plasmid to correct for variable transfection efficiencies. PUC19 carrier DNA was added to a total of 15 μg (L691, NIH 3T3, MC 3T3 and KM1/K3), 10 μg (MPC11) or 8 μg (NALM6) of DNA pr. transfection. All transfections were done in duplicate and repeated three to eleven times. CAT and luciferase assays were performed as described earlier (Ethelberg et al., 1997a).

PCR and DNA sequencing analysis

Provirus LTR sequences were amplified from gDNA of NIH 3T3 virus-producing cell lines and mouse tumor tissues using primers 440 (5′-TTCATAAGGCTTAGCCAGC-TAACTGCAG-3′; nucleotide positions 14 to 41 of the Akv1-99 LTR) and 2620 (5′-biotin-*GAATTCGATATC*-GATCCCCGGTCATCTGGG-3′; positions 278 to 261 of the Akv1-99 LTR, with a 12-bp linker added for other purposes (underlined)). In all cases, the PCR gave rise to a single product of the expected size (277-bp). After purification, either on streptavidin-coated magnetic beads (Dynabead M280-streptavidin; Dynal AS, Oslo, Norway) or by using the GFX™ PCR DNA and Gel Band Purification Kit (Amersham Pharmacia Biotech), the amplification products were sequenced on both strands using primers 440 and 2620, as described previously (Lovmand et al., 1998; Sørensen et al., 1993).

Acknowledgments

The technical assistance of Lone Højgaard, Angelika Appold, Katrin Reindl, Jaqueline Müller, Nadine Kink and Elenore Samson is gratefully acknowledged. We thank Dr. Kenneth Alan Howard for critical reading of the manuscript. This work was supported by the Danish Cancer Society, the Novo Nordic Foundation, the Karen Elise Jensen Foundation, the Danish Natural Sciences and Medical Research Councils, and the Nationales Genomforschungsnetz (NGFN).

References

Angel, J.M., Bedigian, H.G., 1984. Expression of murine leukemia viruses in B-cell lymphomas of CWD/Agl mice. J. Virol. 52 (2), 691–694.

Byrd, L.G., McDonald, A.H., Gold, L.G., Potter, M., 1991. Specific pathogen-free BALB/cAn mice are refractory to plasmacytoma induction by pristane. J. Immunol. 147 (10), 3632–3637.

Celander, D., Haseltine, W.A., 1984. Tissue-specific transcription preference as a determinant of cell tropism and leukaemogenic potential of murine retroviruses. Nature 312 (5990), 159–162.

Chatis, P.A., Holland, C.A., Silver, J.E., Frederickson, T.N., Hopkins, N., Hartley, J.W., 1984. A 3′ end fragment encompassing the transcriptional enhancers of nondefective Friend virus confers erythroleukemogenicity on Moloney leukemia virus. J. Virol. 52 (1), 248–254.

Chaudhry, A.Z., Vitullo, A.D., Gronostajski, R.M., 1998. Nuclear factor I (NFI) isoforms differentially activate simple versus complex NFI-responsive promoters. J. Biol. Chem. 273 (29), 18538–18546.

DesGroseillers, L., Jolicoeur, P., 1984. The tandem direct repeats within the long terminal repeat of murine leukemia viruses are the primary determinant of their leukemogenic potential. J. Virol. 52 (3), 945–952.

Ethelberg, S., Hallberg, B., Lovmand, J., Schmidt, J., Luz, A., Grundström, T., Pedersen, F.S., 1997a. Second-site proviral enhancer alterations in lymphomas induced by enhancer mutants of SL3-3 murine leukemia virus: negative effect of nuclear factor 1 binding site. J. Virol. 71 (2), 1196–1206.

Ethelberg, S., Lovmand, J., Schmidt, J., Luz, A., Pedersen, F.S., 1997b. Increased lymphomagenicity and restored disease specificity of AML1 site (core) mutant SL3-3 murine leukemia virus by a second-site enhancer variant evolved in vivo. J. Virol. 71 (10), 7273–7280.

Ethelberg, S., Tzschaschel, B.D., Luz, A., Diaz-Cano, S.J., Pedersen, F.S., Schmidt, J., 1999. Increased induction of osteopetrosis, but unaltered lymphomagenicity, by murine leukemia virus SL3-3 after mutation of a nuclear factor 1 site in the enhancer. J. Virol. 73 (12), 10406–10415.

Gao, B., Kunos, G., 1998. Cell type-specific transcriptional activation and suppression of the alpha1B adrenergic receptor gene middle promoter by nuclear factor 1. J. Biol. Chem. 273 (48), 31784–31787.

Gasparotto, D., De Re, V., Boiocchi, M., 2002. Hepatitis C virus, B-cell proliferation and lymphomas. Leuk. Lymphoma 43 (4), 747–751.

Gilbert, D.J., Neumann, P.E., Taylor, B.A., Jenkins, N.A., Copeland, N.G., 1993. Susceptibility of AKXD recombinant inbred mouse strains to lymphomas. J. Virol. 67 (4), 2083–2090.

Gimbel, W., Schmidt, J., Brack-Werner, R., Luz, A., Strauss, P.G., Erfle, V., Werner, T., 1996. Molecular and pathogenic characterization of the RFB osteoma virus: lack of oncogene and induction of osteoma, osteopetrosis, and lymphoma. Virology 224 (2), 533–538.

Golemis, E.A., Speck, N.A., Hopkins, N., 1990. Alignment of U3 region sequences of mammalian type C viruses: identification of highly conserved motifs and implications for enhancer design. J. Virol. 64 (2), 534–542.

Goyal, N., Knox, J., Gronostajski, R.M., 1990. Analysis of multiple forms of nuclear factor I in human and murine cell lines. Mol. Cell. Biol. 10 (3), 1041–1048.

Gronostajski, R.M., 2000. Roles of the NFI/CTF gene family in transcription and development. Gene 249 (1–2), 31–45.

Hallberg, B., Grundström, T., 1988. Tissue specific sequence motifs in the enhancer of the leukaemogenic mouse retrovirus SL3-3. Nucleic Acids Res. 16 (13), 5927–5944.

Hallberg, B., Schmidt, J., Luz, A., Pedersen, F.S., Grundström, T., 1991. SL3-3 enhancer factor 1 transcriptional activators are required for tumor formation by SL3-3 murine leukemia virus. J. Virol. 65 (8), 4177–4181.

Hartley, J.W., Chattopadhyay, S.K., Lander, M.R., Taddesse-Heath, L., Naghashfar, Z., Morse, H.C., Fredrickson, T.N., 2000. Accelerated appearance of multiple B cell lymphoma types in NFS/N mice congenic for ecotropic murine leukemia viruses. Lab. Invest. 80 (2), 159–169.

Hurwitz, R., Hozier, J., LeBien, T., Minowada, J., Gajl-Peczalska, K., Kubonishi, I., Kersey, J., 1979. Characterization of a leukemic cell line of the pre-B phenotype. Int. J. Cancer 23 (2), 174–180.

Jenkins, N.A., Copeland, N.G., Taylor, B.A., Lee, B.K., 1982. Organization, distribution, and stability of endogenous ecotropic murine leukemia virus DNA sequences in chromosomes of Mus musculus. J. Virol. 43 (1), 26–36.

Kruse, U., Sippel, A.E., 1994. The genes for transcription factor nuclear factor I give rise to corresponding splice variants between vertebrate species. J. Mol. Biol. 238 (5), 860–865.

Kuehl, W.M., Bergsagel, P.L., 2002. Multiple myeloma: evolving genetic events and host interactions. Nat. Rev., Cancer 2 (3), 175–187.

Lawrenz-Smith, S.C., Massey, A.C., Innes, D.J., Thomas, C.Y., 1994. Pathogenic determinants in the U3 region of recombinant murine leukemia viruses isolated from CWD and HRS/J mice. J. Virol. 68 (8), 5174–5183.

Leib-Mösch, C., Schmidt, J., Etzerodt, M., Pedersen, F., Hehlmann, R., Erfle, V., 1986. Oncogenic retrovirus from spontaneous murine osteomas: II. Molecular cloning and genomic characterization. Virology 150, 96–105.

Lenz, J., Celander, D., Crowther, R.L., Patarca, R., Perkins, D.W., Haseltine, W.A., 1984. Determination of the leukaemogenicity of a murine retrovirus by sequences within the long terminal repeat. Nature 308 (5958), 467–470.

Lovmand, J., 1996. PhD thesis. Aarhus University, Denmark.

Lovmand, S., Kjeldgaard, N.O., Jørgensen, P., Pedersen, F.S., 1990. Enhancer functions in U3 of Akv virus: a role for cooperativity of a tandem repeat unit and its flanking DNA sequences. J. Virol. 64 (7), 3185–3191.

Lovmand, J., Sørensen, A.B., Schmidt, J., Østergaard, M., Luz, A., Pedersen, F.S., 1998. B-Cell lymphoma induction by Akv murine leukemia viruses harboring one or both copies of the tandem repeat in the U3 enhancer. J. Virol. 72 (7), 5745–5756.

Luz, A., Murray, A.B., Schmidt, J., 1991. Osteoma, spontaneous and virus-induced, mouse. In: Jones, T.C., Mohr, U., Hunt, R.D. (Eds.), Monographs on Pathology of Laboratory Animals. ILSI, Springer, New York, NY.

Mermod, N., O'Neill, E.A., Kelly, T.J., Tjian, R., 1989. The proline-rich transcriptional activator of CTF/NF-I is distinct from the replication and DNA binding domain. Cell 58 (4), 741–753.

Morse III, H.C., Anver, M.R., Fredrickson, T.N., Haines, D.C., Harris, A.W., Harris, N.L., Jaffe, E.S., Kogan, S.C., MacLennan, I.C., Pattengale, P.K., Ward, J.M., 2002. Bethesda proposals for classification of lymphoid neoplasms in mice. Blood 100 (1), 246–258.

Mucenski, M.L., Taylor, B.A., Jenkins, N.A., Copeland, N.G., 1986. AKXD recombinant inbred strains: models for studying the molecular genetic basis of murine lymphomas. Mol. Cell. Biol. 6 (12), 4236–4243.

Mucenski, M.L., Taylor, B.A., Copeland, N.G., Jenkins, N.A., 1987. Characterization of somatically acquired ecotropic and mink cell focus-forming viruses in lymphomas of AKXD recombinant inbred mice. J. Virol. 61 (9), 2929–2933.

Mucenski, M.L., Bedigian, H.G., Shull, M.M., Copeland, N.G., Jenkins, N.A., 1988. Comparative molecular genetic analysis of lymphomas from six inbred mouse strains. J. Virol. 62 (3), 839–846.

Mundy, G.R., 1997. Mechanisms of bone metastasis. Cancer 80 (8 Suppl), 1546–1556.

Murray, A.B., Schmidt, J., Luz, A., 1991. Osteopetrosis induced by retrovirus, mouse. In: Jones, T.C., Mohr, U., Hunt, R.D. (Eds.), Monographs on Pathology of Laboratory Animals. ILSI, Springer, New York, NY, pp. 284–291.

Nieves, A., Levy, L.S., Lenz, J., 1997. Importance of a c-Myb binding site for lymphomagenesis by the retrovirus SL3-3. J. Virol. 71 (2), 1213–1219.

Olsen, H.S., Lovmand, S., Lovmand, J., Jørgensen, P., Kjeldgaard, N.O., Pedersen, F.S., 1990. Involvement of nuclear factor I-binding sites in control of Akv virus gene expression. J. Virol. 64 (9), 4152–4161.

Østergaard, M., Pedersen, L., Schmidt, J., Luz, A., Lovmand, J., Erfle, V., Pedersen, F.S., Strauss, P.G., 1997. Mapping of a major osteomagenic determinant of murine leukemia virus RFB-14 to non-long terminal repeat sequences. J. Virol. 71 (1), 645–649.

Potter, M., Wax, J.S., 1983. Peritoneal plasmacytomagenesis in mice: comparison of different pristane dose regimens. J. Natl. Cancer Inst. 71 (2), 391–395.

Potter, M., Wiener, F., 1992. Plasmacytomagenesis in mice: model of neoplastic development dependent upon chromosomal translocations. Carcinogenesis 13 (10), 1681–1697.

Potter, M., Hartley, J.W., Wax, J.S., Gallahan, D., 1984. Effect of MuLV-related genes on plasmacytomagenesis in BALB/c mice. J. Exp. Med. 160 (2), 435–440.

Roodman, G.D., 1997. Mechanisms of bone lesions in multiple myeloma and lymphoma. Cancer 80 (8), S1557–S1563.

Rosner, A., Peled, A., Haran-Ghera, N., Canaani, E., 1993. Analysis of Ly-1$^+$ B-cell populations of IgH rearrangements in "normal" spleens and in lymphomas of AKR/J and AKV Fv-1b mice. Cancer Res. 53, 2147–2153.

Schmidt, J., Erfle, V., Pedersen, F.S., Rohmer, H., Schetters, H., Marquart, K.H., Luz, A., 1984. Oncogenic retrovirus from spontaneous murine osteomas: I. Isolation and biological characterization. J. Gen. Virol. 65 (Pt. 12), 2237–2248.

Schmidt, J., Luz, A., Erfle, V., 1988. Endogenous murine leukemia viruses: frequency of radiation-activation and novel pathogenic effects of viral isolates. Leuk. Res. 12 (5), 393–403.

Schmidt, J., Krump-Konvalinkova, V., Luz, A., Goralczyk, R., Snell, G., Wendel, S., Dorn, S., Pedersen, L., Strauss, P.G., Erfle, V., 1995. Akv murine leukemia virus enhances bone tumorigenesis in hMT-c-fos-LTR transgenic mice. Virology 206 (1), 85–92.

Schmidt, J., Lumniczky, K., Tzschaschel, B.D., Guenther, H.L., Luz, A., Riemann, S., Gimbel, W., Erfle, V., Erben, R.G., 1999. Onset and dynamics of osteosclerosis in mice induced by Reilly–Finkel–Biskis (RFB) murine leukemia virus. Increase in bone mass precedes lymphomagenesis. Am. J. Pathol. 155 (2), 557–570.

Sørensen, A.B., Duch, M., Jørgensen, P., Pedersen, F.S., 1993. Amplification and sequence analysis of DNA flanking integrated proviruses by a simple two-step polymerase chain reaction method. J. Virol. 67 (12), 7118–7124.

Speck, N.A., Renjifo, B., Golemis, E., Fredrickson, T.N., Hartley, J.W., Hopkins, N., 1990. Mutation of the core or adjacent LVb elements of the Moloney murine leukemia virus enhancer alters disease specificity. Genes Dev. 4 (2), 233–242.

Speth, C., Luz, A., Strauss, P.G., Wendel, S., Zeidler, R., Dorn, S., Erfle, V., Brem, G., Lipp, M., Schmidt, J., 1995. Akv murine leukemia virus enhances lymphomagenesis in myc-kappa transgenic and in wild-type mice. Virology 206 (1), 93–99.

Stall, A.M., Farinas, M.C., Tarlinton, D.M., Lalor, P.A., Herzenberg, L.A., Strober, S., 1988. Ly-1 B-cell clones similar to human chronic lymphocytic leukemias routinely develop in older normal mice and young autoimmune (New Zealand Black-related) animals. Proc. Natl. Acad. Sci. U.S.A. 85 (19), 7312–7316.

Sudo, H., Kodama, H.A., Amagai, Y., Yamamoto, S., Kasai, S., 1983. In vitro differentiation and calcification in a new clonal osteogenic cell line derived from newborn mouse calvaria. J. Cell Biol. 96 (1), 191–198.

Tarlinton, D., Stall, A., Herzenberg, L., 1988. Repetitive usage of immunoglobulin VH and D gene segments in CD5$^+$ Ly-1 B clones of (NZB x NZW)F1 mice. EMBO J. 7 (12), 3705–3710.

Weng, W.K., Levy, S., 2003. Hepatitis C virus (HCV) and lymphomagenesis. Leuk. Lymphoma 44 (7), 1113–1120.

Werenskiold, A.K., Rossler, U., Lowel, M., Schmidt, J., Heermeier, K., Spanner, M.T., Strauss, P.G., 1995. Bone matrix deposition of T1, a homologue of interleukin 1 receptors. Cell Growth Differ. 6 (2), 171–177.

Whyte, M., 1996. Sclerosing bone dysplasias. Primer on the metabolic bone diseases and disorders of mineral metabolism, 3rd ed. Lippincott-Raven, Philadelphia, PA, pp. 363–387.

Yamada, Y., Matsushiro, H., Ogawa, M.S., Okamoto, K., Nakakuki, Y., Toyokuni, S., Fukumoto, M., Hiai, H., 1994. Genetic predisposition to pre-B lymphomas in SL/Kh strain mice. Cancer Res. 54 (2), 403–407.